Liquid Crystal Auto-Induction and Amplification Function for Circularly Polarized Luminescence (CPL) with High g_{em}-Value, and Dynamically Controllable CPL Devices

Hiromasa Goto
Correspondence to H. Goto, e-mail: gotoh@ims.tsukuba.ac.jp

Department of Materials Sciences, Faculty of Pure and Applied Sciences,
University of Tsukuba, Tsukuba, Ibaraki 305-8573, Japan

Keywords: Auto-chiral induction; CPL amplification; dynamic switching of CPL; intense g_{em}; 3D helical collective.

Abstract
Optically active phenylenevinylene derivatives with fluorescence are employed for preparation of a cholesteric liquid crystal based circularly polarized light (CPL) emission device. The device shows intense CPL with a quite large value of the g_{em}-factor (= 0.6) and quick CPL light switching driven by cholesteric-nematic transition with a homeotropic alignment. This research develops the auto-induction of fluorescent chiral inducers in host liquid crystal for formation of a helical structure with CPL amplification. The present research applies a classical LC light-scattering system using chiral technology as a new method for obtaining CPL dynamic control with an intense g_{em}-factor.

1. Introduction

Freedericksz transition is external electric field driven change in molecular orientation of nematic liquid crystals (LC). The nematic molecule is quickly oriented in the normal direction to the substrate from random with application of voltage. The orientation change functions as a dynamically controllable light shutter. Previously, we reported optical rotation LC devices. The device shows dynamically controllable large optical rotation (5.7 x 10^4 deg/mm) [1]. The change in optical rotation of the LC device is driven by a change in molecular alignment. Helical structure based materials show quite high optical rotation and intense circular dichroism. Application of electric field for the LC device allows cholesteric-nematic change accompanied by unwinding of helicity followed by perpendicular orientation against the substrate. In this case, incident light can be passed through with no modulation.

Polypeptides having a fluorescence chromophore in the substituent show circularly polarized luminescence (CPL) [2]. Previously, we have found green fluorescent protein (GFP) emits circularly polarized light [3]. These results indicate that natural micro-organisms can emit CPL. Furthermore, some fishes such as lantern-eye fish show a flashing sign in the sea, implying CPL from the fish can blink on and off.

In this research, dynamic control of CPL from LC devices is reported. Addition of a small amount of chiral inducer (chiral dopant) to achiral nematic LC allows formation of cholesteric LC having a helical structure, Figure 1. Although quasi-layers are added to this cholesteric LC model in Figure 1, the cholesteric phase (Ch*) (chiral nematic

phase) has no layer structures. Fundamentally, cholesteric LC and nematic LC have the same molecular order, although cholesteric LC with small helical pitch show a SmA-like fan-shaped texture. The fan-shaped texture of the cholesteric phase may be referred to as a quasi domain. Cholesteric-nematic change by unwinding of the helical structure [4] is induced by shear flow [5], magnetic field [5], and electric field [6].

The chiral inducers employed in this study have both optical activity and fluorescence, resulting in circularly polarized light emission. A cholesteric LC with a 3D helical structure produced by addition of the chiral inducers to nematic LC shows amplified CPL with a large g_{em} dissymmetry factor. Application of a pulse electric field against the LC device based on this fluorescent cholesteric LC allows flashing of CPL. This report is the first example of preparation of an LC-based high-efficiency circularly polarized emission device with quick control.
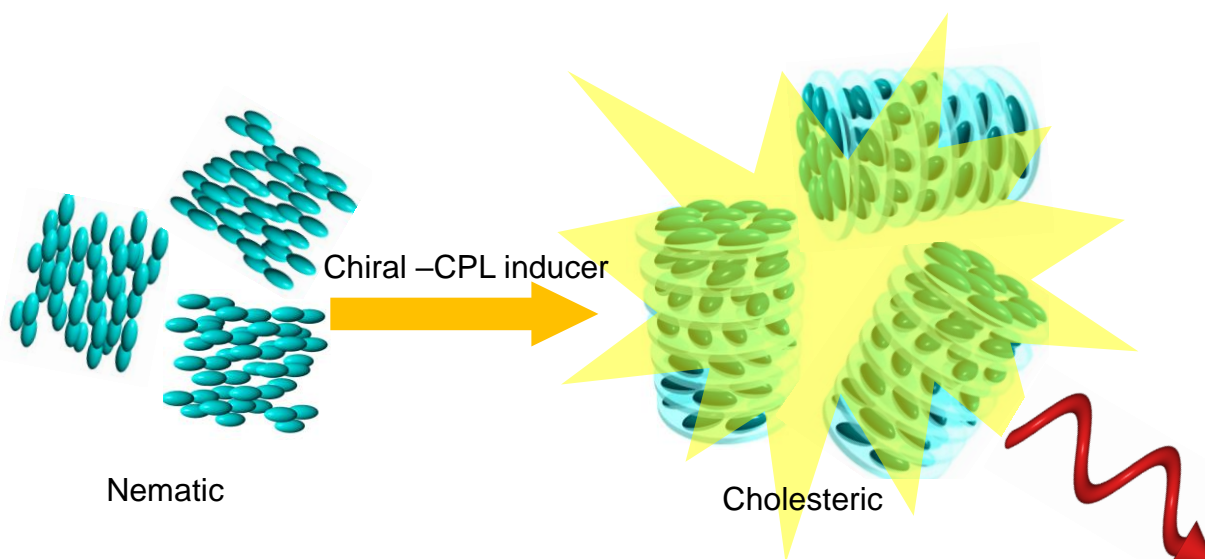
Figure 1. Induction of the cholesteric phase and circularly polarized emission by addition of fluorescent chiral inducers.

2. Experimental

Constituents of chemical structures of the chiral inducers (dopants) denoted as (+)-1, (−)-2, (−)-3, (−)-4 ("+" and "−" are optical rotation directions), and host LC (4-cyano-4'-pentylbiphenyl, 5CB) in the LC system are shown in Figure 2 [1]. The chiral inducers and the CPL devices were prepared by a previously reported method. Fourier transform infrared (FT-IR) spectroscopy measurements and NMR measurements confirm the chemical structure of the guest compounds. The IR spectroscopy measurements show absorption bands due to C-H stretching of alkyl groups at around 2900 and 2860 cm^{-1}. An absorption of C=O stretching was observed at 1713 cm^{-1}. An absorption of C=C stretching of phenylene rings was confirmed at 1600 cm^{-1}. ^{1}H NMR of the compound (+)-1 in CDCl$_3$ solution reveals absorptions due to protons at the stereogenic center at 5.17 ppm from tetramethyl silane (TMS, internal standard) as a sextet signal. Protons on phenylene groups appear at a low magnetic region at 7.13-7.25, 7.54-7.64, and 8.03 ppm from TMS. ^{1}H NMR of the compound

(−)-3 shows multiplet signals due to protons at stereogenic centers. The NMR data of
the compound are summarized in Table 1 [1].

CPL device	Guest	Host[1]
PV-RR	(+)-1	5CB
PV-SS	(−)-2	5CB
PV-SRS	(−)-3	5CB
PV-SSS	(−)-4	5CB
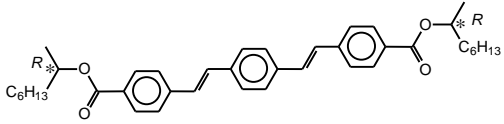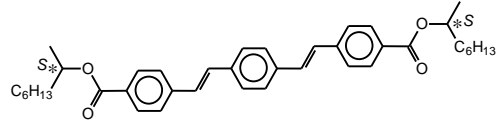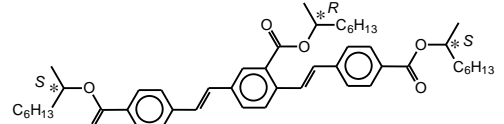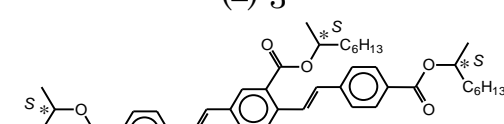
[1]5CB :
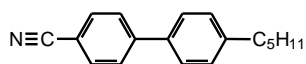
Figure 2. Constituents of the circularly polarized luminescence device. * = stereogenic
center. (+) and (−) are optical rotation directions.

Table 1. ^{1}H NMR signals of chiral inducers.

^{1}H signals in NMR[a,b]	(+)-1	(−)-2	(−)-3	(−)-4
-C$\underline{H}_3$	0.88 (t)	0.88 (t)	0.86-0.96 (m)	0.86-0.94 (m)
-OC*HC$\underline{H}_3$CH$_2$ (C$\underline{H}_2$)$_4$CH$_3$	1.28-1.39	1.29-1.37	1.25-1.41	1.25-1.41
-OC*HCH$_3$C$\underline{H}_2$(CH$_2$)$_4$CH$_3$	1.54-1.76	1.54-1.79	1.55-1.79	1.55-1.79
-OC*$\underline{H}$CH$_3$	5.17 (s)	5.17 (s)	5.13-5.19 (m)	5.13-5.19 (m)
Phenyl protons	7.13-7.25, 7.54-7.64, 8.03 (d)	7.41-7.26, 7.55-7.72, 8.03 (d)	7.50-7.77, 8.01-8.09 (m)	7.50-7.77, 8.01-8.09 (m)

[a]δ from tetramethyl silane (TMS) in CDCl$_3$, ppm, 270 MHz ^{1}H NMR.
[b] (t) = triplet, (s) = sextet, (d) = doublet, (m) = multiplet.

1/100 equivalent mole amount of the chiral inducer (guest molecule) was added to the host nematic LC. The mixture was heated in a vial to completely dissolve the chiral inducer in 5CB. Visual inspection confirmed formation of a homogeneous LC solution. The mixture shows the cholesteric phase at rt. under polarizing optical microscopy (POM) observation.

A POM image of PV-RR/5CB at 20 °C is shown in Figure 3. The mixture exhibits a fine striped fan-shaped texture due to formation of the cholesteric phase.
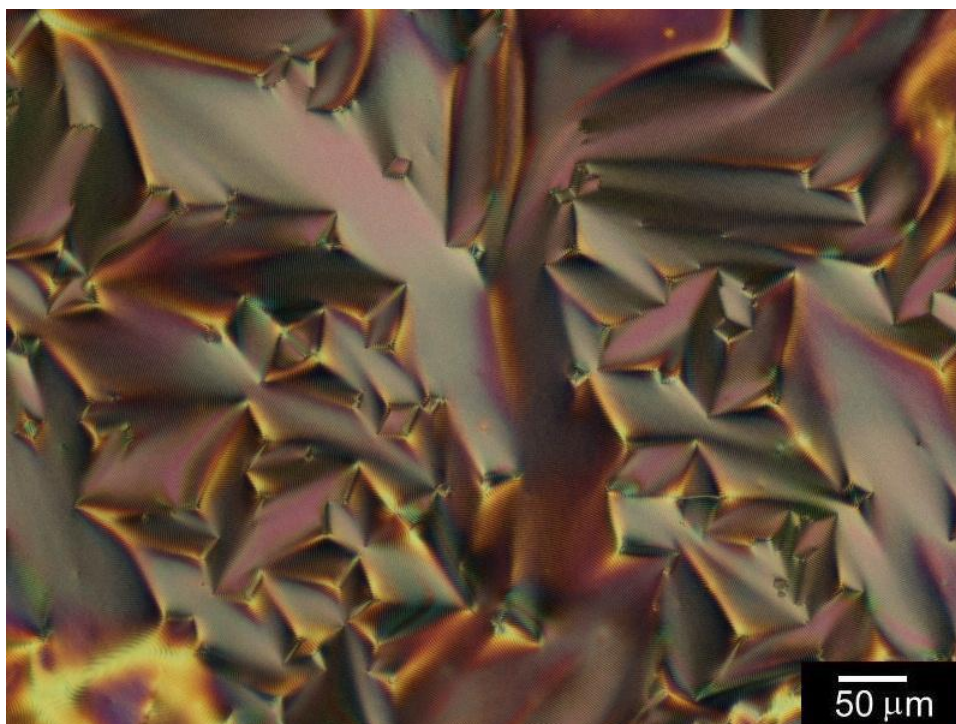
Figure 3. Polarizing optical microscopy image of a cholesteric liquid crystal mixture ((+)-1/5CB) showing a cholesteric fan-shaped texture. Magnification: 100 x.

Preparation of the LC cell was then carried out by injecting the isotropic state mixture (PVs/5CB) between indium tin oxide (ITO) coated glass electrodes (9 Ω cm^{-2}, ca. 12 nm thick) using a polyvinylidene chloride sheet (12 μm thick) as a spacer. The reaction cell was heated to 40 °C and then gradually cooled to 25 °C. The LC devices are denoted as PV-RR, PV-SS, PV-SRS, and PV-SSS, Figure 2.

A high-frequency rectangular wave (200 Hz, 5 V) was generated using a function generator. The rectangular wave voltage was periodically (ON-OFF) applied to the LC device via a custom-made relay drive circuit with low frequency. The entire circuit for application of an electric field to the CPL device is shown in Figure 4(a). Figures 4(a-1, a-2) display an electric relay drive for switching (0.1-1 Hz) and a function generator (200 Hz). Figure 4(b) shows the custom-made electric relay device. A high frequency produced by the function generator is periodically applied to the cell with the electric relay device. The waveform of the electric field for the LC cell is described in Figure 4(c). Figure 4(d) shows the LC-CPL device.

4
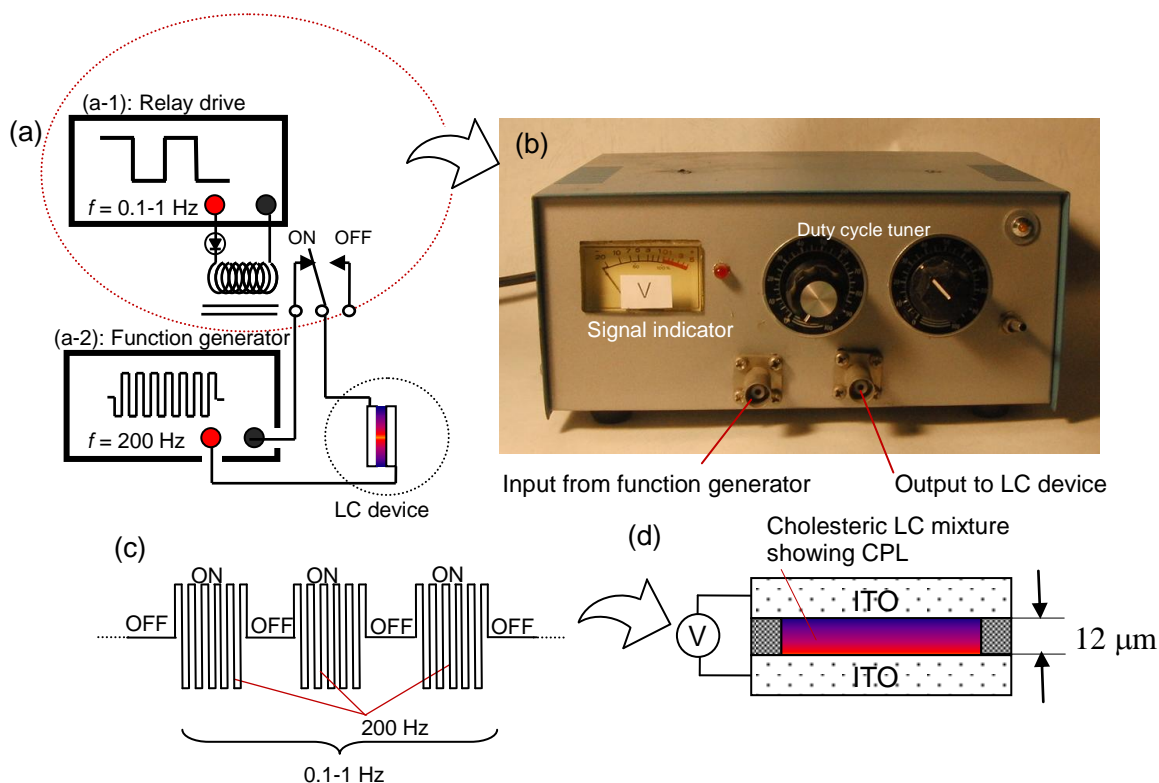
Figure 4. (a): Entire circuit for application of an electric field to the CPL device. Electric relay for switching (0.1-1 Hz), and function generator (200 Hz). (b): Custom-made electric relay device. (c): Applied waveform for the LC cell. (d): LC-CPL device. ITO = indium-tin-oxide-coated conducting glass.

The radiative transition probabilities for left (L) and right (R) photons in the spontaneous emission are unequal in chiral molecules,

$$\Delta I = I_L - I_R. \quad (1)$$

The average luminescence intensity is expressed by

$$I = (I_L + I_R)/2. \quad (2)$$

The degree of circular polarization in the emission is defined by

$$g_{em} = 2\Delta I/I = 2(I_L - I_R)/(I_L + I_R) = I_{CPL}/I_{PL} \quad (3)$$

where g_{em}, V_{DC}, V_{AC}, I_{CPL}, and I_{PL} are the dissymmetry factor in the emission, measured fluorescence and CPL, intensity of CPL, and intensity of PL, respectively [7].

Figure 5 shows CPL spectroscopy measurement results of the PV-RR and PV-SS as CPL devices. PV-RR shows fluorescence at 440 nm upon irradiation of 335 nm as an excitation light. Application of an electric field across the LC device decreases the intensity of the fluorescence. This can be due to a change from the cholesteric to the

nematic phase and subsequent homeotropic alignment.

Here, change from the cholesteric to the nematic phase is not a phase transition because the cholesteric phase is basically the same as the nematic. The twist angle between adjacent molecules is quite small. The angle is almost zero relative to that of the nematic phase. Accumulation of a small twist angle between adjacent molecules forms a visually observable long helical pitch. The CPL measurements reveal that g_{em}-factors of the PV-RR and PV-SS devices are -0.6 and 0.38, quite large, respectively. The CPL spectra and g_{em}-factor of the PV-RR and PV-SS devices are complementary mirror images and opposite values, respectively, indicating these CPL signals are the original CPL emission [8].
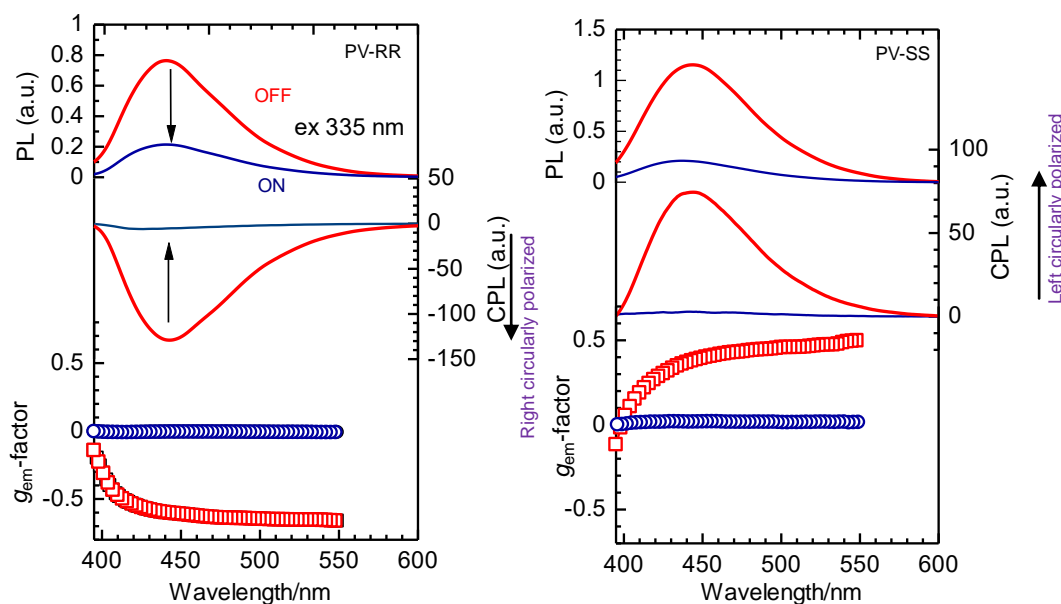
Figure 5. Photoluminescence (PL), circular polarized luminescence (CPL) emission spectroscopy, and dissymmetry factor of emission (g_{em}) measurement results of the PV-RR and PV-SS. Top: Photoluminescence (PL). Middle: Circularly polarized emission. Bottom: Dissymmetry factor in the emission. Red lines and squares: PL, CPL and dissymmetry factor with no application of voltage across the LC device (OFF). Blue lines and squares: PL, CPL and dissymmetry factor with application of voltage across the LC device (ON).

(+)-1 in chloroform solution shows a CPL signal at 423 nm with a g_{em}-factor of -2.34 x 10^{-4} (449 nm), while the PV-RR device consisting of (+)-1 in 5CB matrix shows a negative CPL signal as a trough at 440 nm (g_{em} = - 0.6) due to formation of a 3D helical structure in the cholesteric phase amplifying the g_{em} value ca. 2500-fold.

The random orientation of the helical axis of the LC shows CPL (no applied voltage). This mechanism is comparable to LC dynamic scattering [9]. On the other hand, the light passes through the parallel oriented molecules to the optical axis under application of an electric field. In this case, the chiral fluorescent molecules in the matrix LC have no excitation by incident light, resulting in no CPL under the electric field, accompanied by a change from the cholesteric to the oriented nematic phase. Conoscopic observation of the device with an electric field confirms the LC molecules

orient along the incident light axis [1]. These results demonstrate that the LC device functions as an electric field driven CPL driver based on change in helix-uniaxial molecular orientation and homeotropic alignment of the molecule.
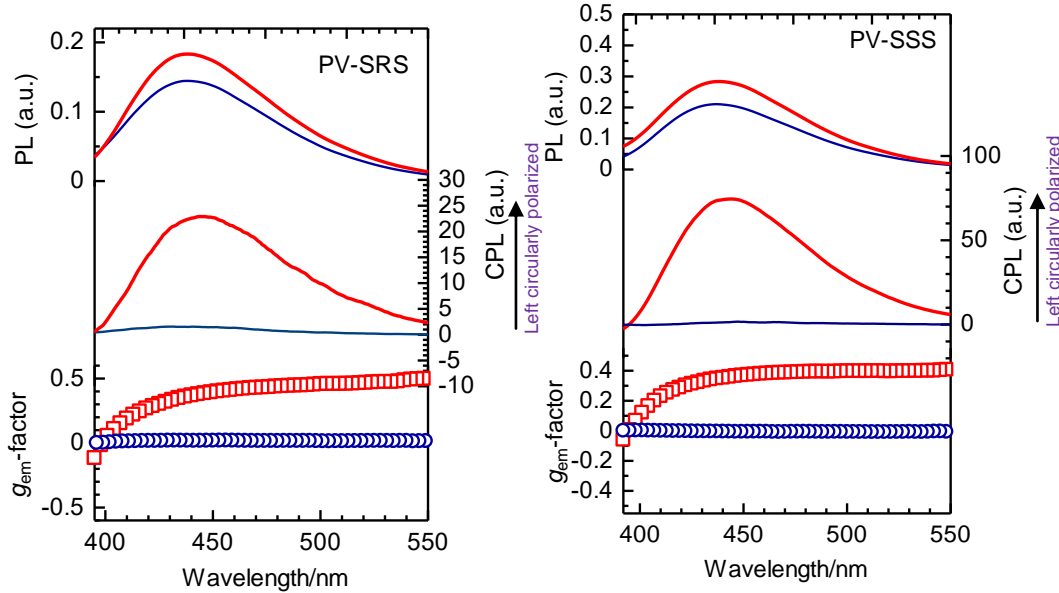
Figure 6. PL, CPL spectroscopy, and dissymmetry factor of emission (g_{em}) measurement results of the PV-SRS and PV-SSS. Top: Photoluminescence (PL). Middle: Circularly polarized emission. Bottom: Dissymmetry factor in the emission. Red lines and squares: PL, CPL and dissymmetry factor with no application of voltage across the LC device (OFF). Blue lines and squares: PL, CPL and dissymmetry factor with application of voltage across the LC device (ON).

Figure 6 shows PL and CPL emission spectroscopy measurement results of PV-SRS and PV-SSS CPL devices. PV-SRS and PV-SSS show fluorescence at 437 and 438 nm, respectively. Application of an electric field across the LC device decreases the intensity of the fluorescence. However, large anisotropy in the PL was not obtained due to the branched structure of the CPL inducer in the 5CB matrix. A slight mechanical fluctuation of the molecules may still exist after the alignment. Further application of high voltage to the cell may improve anisotropy. PV-SRS and PV-SSS show a left-handed CPL signal with no application of voltage to the LC device (0 V, OFF). Application of an electric field allows a decrease of the CPL intensity. g_{em}-Factors of the PV-SRS and PV-SSS devices are –0.395 and –0.36, respectively. Optical anisotropy of the LC devices upon application of voltage and no voltage are summarized in Table 2.

Table 2. Optical anisotropy of the LC devices upon application of voltage and no voltage.

LC device	Optical anisotropy[1]			
	PL[1]	CPL[1]	g_{em}-Factor[1]	g_{em}-Factor$_{E0}$[2]
PV-RR	3.6 (440 nm)	24.4 (441 nm)	86.7 (441 nm)	-6.0×10^{-1} (441 nm)
PV-SS	5.6 (443 nm)	26.6 (443 nm)	21.1 (443 nm)	3.8×10^{-1} (443 nm)
PV-SRS	1.3 (437 nm)	15.5 (445 nm)	22.3 (445 nm)	-3.9×10^{-1} (445 nm)
PV-SSS	1.4 (438 nm)	53.1 (443 nm)	71.8 (443 nm)	-3.6×10^{-1} (443 nm)

[1]I_0/I_{AP} (I_0 = intensity under zero electric field, I_{AP} = intensity under electric field).
[2]g_{em}-factor under zero electric field.

3. Results and discussion

Chromophores show intense CPL due to a helical aggregation structure in cholesteric LC, although the CPL is derived from no individual molecular asymmetry [8]. Therefore, the CPL of this device comes from structural chirality. Note that the chiral phenylenevinylene compounds show no liquid crystallinity. Although the phenylenevinylene molecules used in this study show weak CPL, chiral induction of the host molecule and the entire system shows quite intense CPL due to the helical structure of the cholesteric phase. The inducer changes the entire environment and emits intense circularly polarized light. In other words, the inducer changes its circumstances and strengthens its performance. This function can be referred to as "auto-induction of chirality". The auto-induction amplifies CPL through formation of a helical structure induced by the molecule itself.

The CPL devices emit CPL under no electric field, Figure 7(a). Application of voltage unwinds the helical twist, Figure 7(b). Finally, homeotropic alignment accompanied by cholesteric-nematic transition permits it to pass through incident light with no light modulation, Figure 7(c). This process allows CPL switching with an electric field. Intense CPL has been founded in metal complexes [11], gels [12], and composites [13]. Nano-crystals show intense CPL [15]. Molecular assembly can be an important point to obtain strong CPL materials. Self-assembly of a light-emitting chiral conjugated polymer has been developed with a cholesteric form [14]. This EL device can perform dynamical switching of CPL light with high efficiency.

The present research applies a classical LC light scattering system using chiral technology as a new method.

4. Conclusion

Auto-chiral induction of a chiral inducer amplifies its own CPL intensity through formation of the cholesteric phase as a form of 3D helical collective. Dynamic switching of the liquid crystal CPL device is driven by helix–non-helix change and subsequent homeotropic orientation. The liquid crystal CPL devices developed in this study perform optical conversion from omni-directional light (non-polarized light) to

circularly polarized light with quick switching due to the low viscosity of the mix LC system. This may be a new type of "chiral dynamic scattering type LC device" showing intense circular polarized light emission.
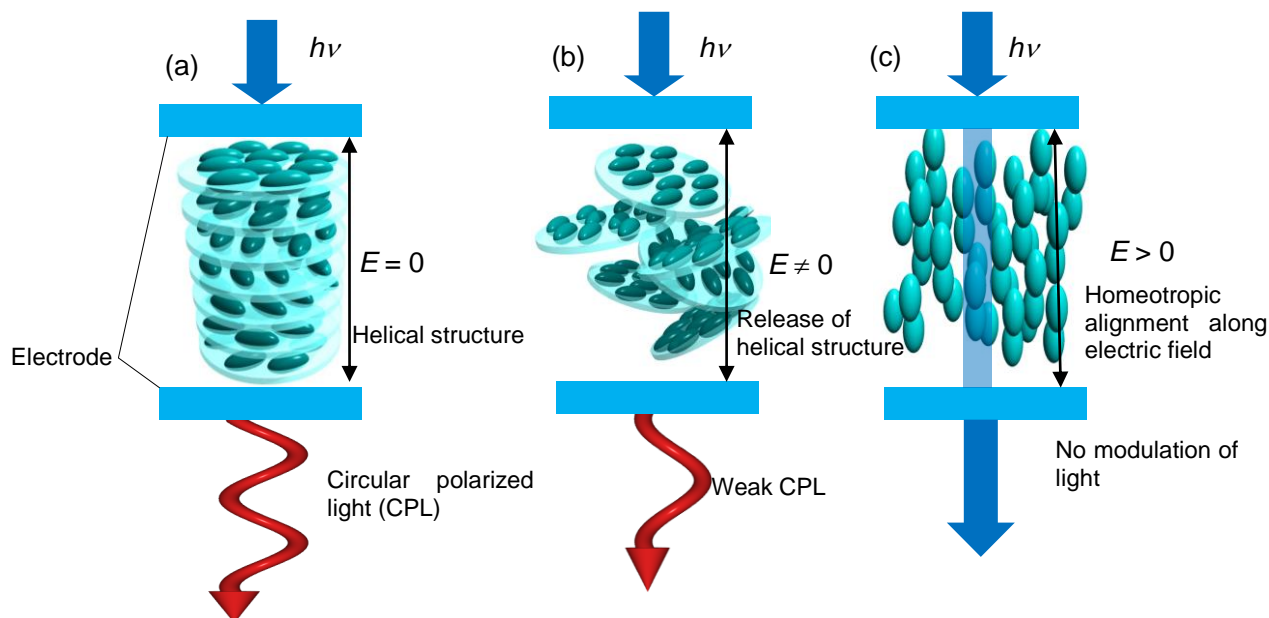
Figure 7. Electrically driven change in circularly polarized light of a liquid crystal device through a change in molecular alignment (cholesteric to nematic, and homeotropic alignment). (a) A zero electric field maintains the helicity of a cholesteric liquid crystal, showing circularly polarized light as output. (b) Application of a low electric field unwinds the helicity of the cholesteric liquid crystal, showing weak circular polarization of the output light. (c) Application of an electric field allows the formation of a homeotropic orientation (perpendicular orientation against the substrate) of liquid crystal molecules, resulting in no modulation of light. Quasi-layers of cholesteric LC are added to show the expression visually, although cholesteric LC form no layer structures, actually.

Instruments

All optical measurements were carried out at 25 °C. A custom-made function generator 1 and a METEX MXG-9802A function generator were used for optical switching. CD spectra were obtained with a JASCO J-720 spectrometer. PL and CPL measurements of the polymers were carried out with a JASCO CPL 200S spectrometer. Optical texture observations were made using a Nikon ECLIPS E 400 POL polarizing optical microscope.

Acknowledgment

Hiromasa Goto,
Liquid Crystal Auto-Induction and Amplification Function for Circularly Polarized Luminescence (CPL)
with High g_{em}-Value, and Dynamically Controllable CPL Devices
Molecular Crystals and Liquid crystals,   669, 1, 27-35 (2019)

Reference

[1] Goto, H., & Kawabata, K. (2013) *J. Disp. Sci. Tech.*, *34*, 311.

[2] Shisido, M., Egusa, S., & Imanishi, Y. (1983) *J. Am. Chem. Soc.*, *105*, 1041.

[3] Goto, H., Sawada, I., & Nomura N. (2010) *Int. J. Polym. Mater.*, *59*,786.

[4] Barbero G., & Scarfone, A. M. (2013) *Phys. Rev. E*, *88*, 03250.

[5] Zakhlevnykh, A.N., Makarov, D.V. & Novikov, A.A. (2017) *J. Exp. Theor. Phys*. *125*, 679.

[6] Swisher, R. R. (1999), *Liq. Cryst.*, 26.

[7] Goto, H. (2007) *Macromolecules*, *40*, 1377.

[8] Shishido, M. (1992) *Jasco rep.*, *34*, 1.

[9] Heilmeier, G. H., & Zanoni, L. A. (1968). *Appl. Phys. Lett.*, *13*, 91.

[10] Sisido, M., Takeuchi, K., & Imanishi, Y. (1983) *Chem. Lett.*, 961-963.

[11] Lunkley, L., Shirotani, D., Yamanari, K.,   Kaizaki, S., & Muller, G. (2008) *J. Am. Chem. Soc.*, *130*, 13814.

[12] Shen, Z., Wang, T., Shi, L., Tang, Z., & Liu, M. (2015) *Chem. Sci.*, *6*, 4267.

[13] Yang, D., Duan, P., Zhang, L., & Liu, M. (2017) *Nature Commun.*, *8*, A15727.

[14] Nuzzo, D. D., Kulkarni, C., Zhao, B., Smolinsky, E., Tassinari, F., Meskers, S. C. J., Naaman, R., Meijer, E. W., & Friend, R. H. (2017) *ACS Nano*, *11*, 12713.

[15] Cheng, J., Hao, J., Liu, H., Li, J., Li, J., Zhu, X., Lin, X., Wang, K., & He, T. (2018) *ACS Nano*, *12*, 5341.

[16] Tohgha, U., Deol, K. K., Porter, A. G., Bartko, S. G., Choi, J. K., Leonard, B. M., Varga, K., Kubelka, J., Muller, G., & Balaz, M. (2013) *ACS Nano*, *7*, 11094.